Supporting Information

An HPQ-based near-infrared dye for the detection of ClO^- and accurate imaging of cell and mouse tumor sites in situ

Lu Zhang, Xue Yao, Min Peng, Yu Ma, Yu Peng*, and Ya-Wen Wang*

School of Chemistry & School of Life Science and Engineering, Key Laboratory of Advanced Technologies of Material Ministry of Education, Southwest Jiaotong University, Chengdu 610031, People's Republic of China

pengyu@swjtu.edu.cn; ywwang@swjtu.edu.cn

Table of Contents

1. General Methods.

Isophorone, malondicyanide, N, N-diisopropylethanamine, trifluoroacetic acid, ρ-Toluenesulfonic acid monohydrate and 2,3-Dichloro-5,6-dicyano-p-benzoquinone and other analytical reagents were all purchased from Innochem Technology Co., Ltd. Deionized water was used in analysis experiments.

The ^{1}H and ^{13}C NMR spectra were recorded on a Bruker AVB-400 spectrometer us ing TMS as the internal reference. HRMS (ESI) spectra were measured with a Waters e2695 spectrometer. Fluorescence spectra were recorded by a F7000 spectrofluorimet er from Hitachi PharmaSpec. Fluorescence imaging of **SWJT-32** in HeLa cells was re corded on a Nikon A1R+ (Japan) laser scanning confocal microscope. Fluorescence i maging of mice was collected on a Xenogen IVIS specturm (Xenogen Corporation, U SA) small animal optical in vivo imaging system.

SWJT-32 was weighed and dissolved in ethanol to prepare 1.0 mM stock solution. Various analytes were dissolved in distilled water or ethanol prepare 0.1 mol/L solution for standby. **SWJT-32** stock solution was diluted to 10.0 μM with EtOH-Tris-HCl (4:6, v/v). For all fluorescence spectra, the excitation was set at 520 nm, the emission wavelength was in the range of 540-700 nm, and the excitation and emission gaps were 10/10 nm.

The quantum yield was calculated through the following formula:

$$\Phi_u = \Phi_s (F_u/F_s)(A_s/A_u)(\eta_u^2/\eta_s^2)$$

"F_u" and "A_u" represent the integral of the fluorescence emission and absorbance spectra of **SWJT-32**, respectively. "F_s" and "A_s" were the integral of the fluorescence emission and absorbance spectra of fluorescein, respectively. "Φ_u" and "Φ_s" represent fluorescence quantum yield of **SWJT-32** and fluorescein, respectively. "η_u" and "η_s" are the refractive index of the solvent of **SWJT-32** and fluorescein, respectively.

The cytotoxicity of **SWJT-32** to HeLa cells was examined by CCK-8 assay method. S3 HeLa cells were seeded at a 96-well culture plate. After growth at 37 ℃ in a 5% CO_2 for 24 h, treated with 0.0, 5.0, 10.0, 15.0, 20.0 μM **SWJT-32**. After incubation for 12 h, the CCK solution was added into each well for further incubation for 4 h.

The absorbance at 540 nm was measured. The HeLa cells were incubated in a glass-bottom petri dish (Φ 15 mm) and adhered at 37 °C for 24 hours. The cells were washed with phosphate buffered saline (PBS) and added 10.0 μM of **SWJT-32** at 37 °C for 30 minutes, then washed with PBS and imaged. After incubating with 200.0 μM ClO^- for 30 min at 37 °C, HeLa cells were washed with PBS and imaged again. HeLa cells were incubated with Nystatin (10.0 μM) or LPS (1.0 μg/mL) for 6 h and then with **SWJT-32** (10.0 μM) for 30 min, then perform other experimental operations. Fluorescence imaging of intracellular **SWJT-32** in HeLa cells was recorded on a laser scanning confocal microscope. The excitation wavelength of the laser is 520 nm.

HeLa cells were injected subcutaneously into 6-week-old BALB/C nude mice to obtain tumor mice models. The other group of tumor mice was injected intravenously with **SWJT-32** (50 μM, 50 μL) and imaged at 0, 1, 2, 3, 4, 5, 6, 7 and 8 h separately. After killing the mice, major organs containing the heart, liver, spleen, lung, kidney, and tumor were dissected and imaged.

All mice were purchased from Chengdu Ensiweier Biotechnology Co., Ltd. and were treated humanely throughout the experiments. Six male mice were used: BALB/C Nude mice (n = 6). At the time of imaging, the mice were 4-8 weeks old and had body weights of 17.2 ± 0.4 g, respectively. This study was approved by the Southwest Military Region General Hospital and Southwest Jiaotong University Animal Experiment Ethics Committee. All animal experiments were conducted and obeyed the Principles of Laboratory Animal Care (People's Republic of China). As controls, one group of mice was only intraperitoneally injected with **SWJT-32** (50 μM, 50 μL) and imaged after 10 min. In the other group, after the mice were intraperitoneally injected with ClO^- (1 mM, 100 μL) and **SWJT-32**(50 μM, 50 μL), they were anesthetized, and the images were obtained at different time points (0, 30, 60, 90, and 120 min).

2. Summary of fluorescent probes for ClO^-

Table. S1

Name	Structure	λ_{em} (nm)	Stokes shift (nm)	LOD (nM)	Mechanism	Reference
BMH-2•Cl	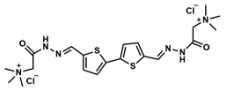	495	55	290	AIE	Ref.188
1	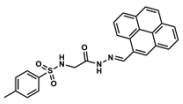	470	55	269	AIE	Ref.19
DBCC	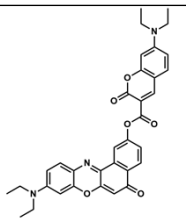	498	128	134	ICT	Ref.20
Hypo-SiF	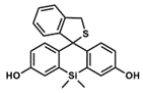	606	20	--	PET	Ref.21
FBS	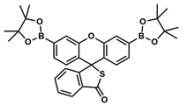	523	25	--ttr	ICT	Ref.22
CVS	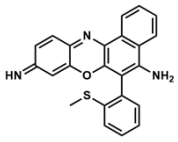	638	42	94.7	PET	Ref.23
CNS	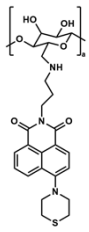	520	80	190	PET	Ref.24

LB	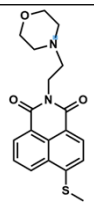	405	55	674	PET	Ref.25
1	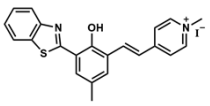	615	155	1.8×10^5	ICT	Ref.26
PHPQ	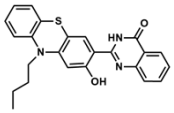	437	98	15	PET	Ref.41
SWJT-32	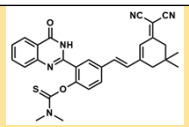	660	**140**	**7.71**	**ESIPT and ICT**	**This work**

3. ^{1}H , ^{13}C NMR, ESI-MS and HRMS copies of SWJT-OH.

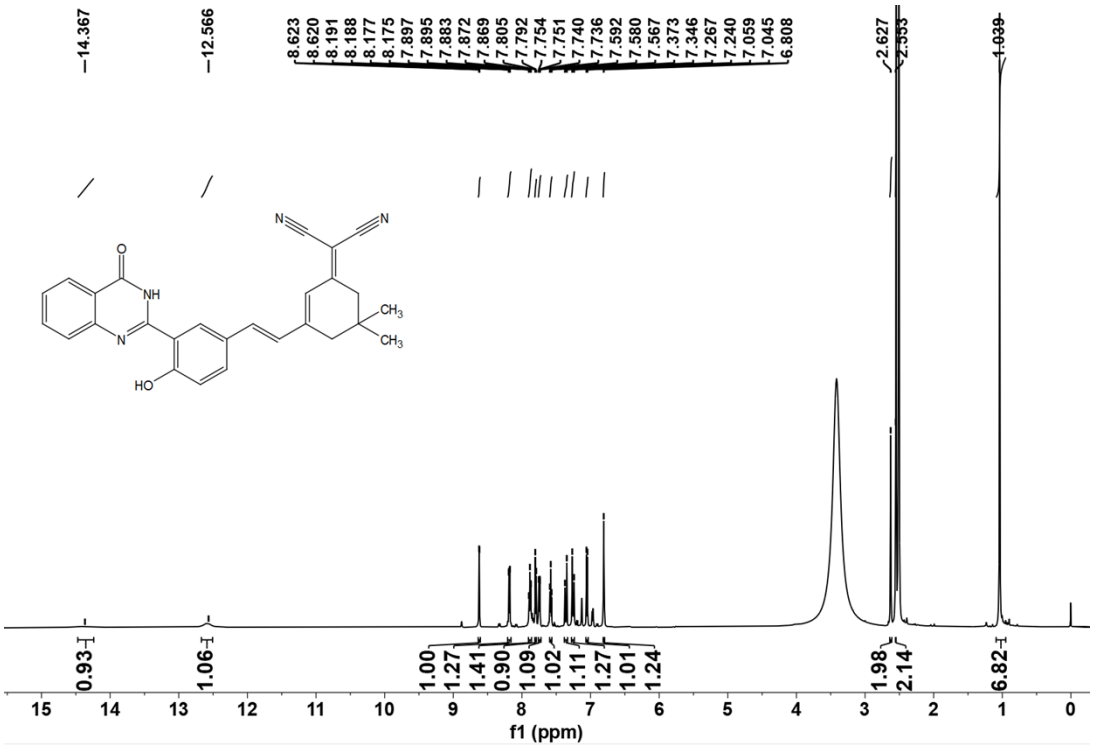

Fig. S1. ^{1}H NMR spectrum of **SWJT-OH** in DMSO-d_6 (400MHz).

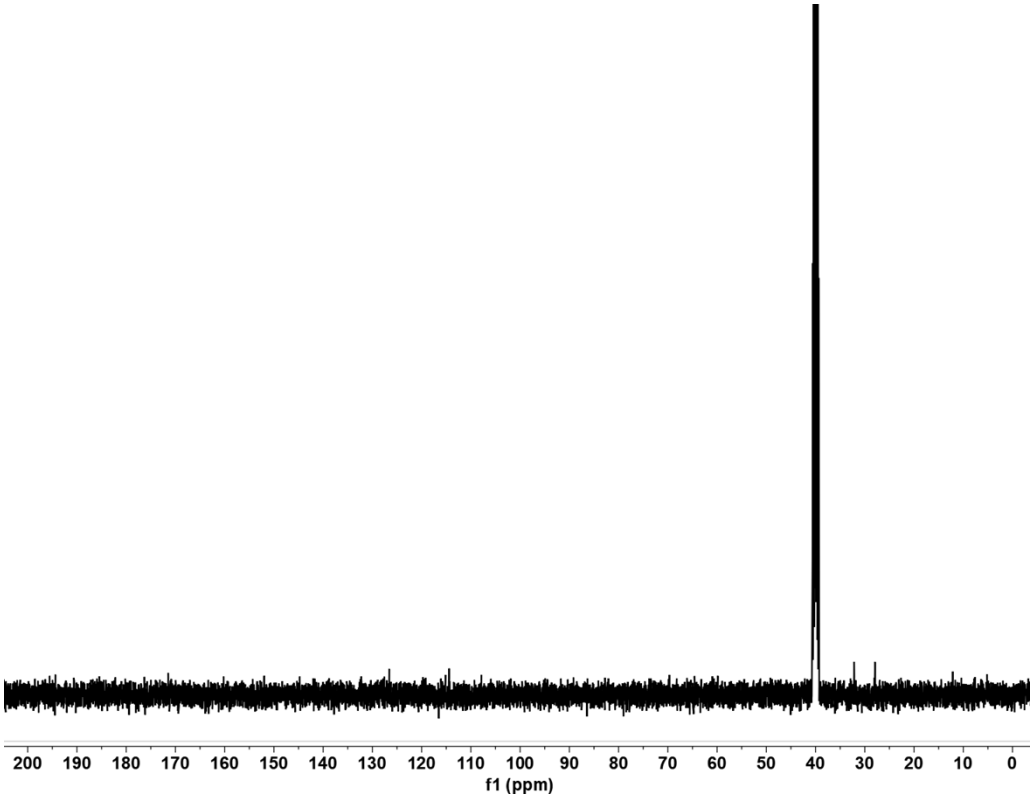

Fig. S2. ^{13}C NMR spectrum of **SWJT-OH**.

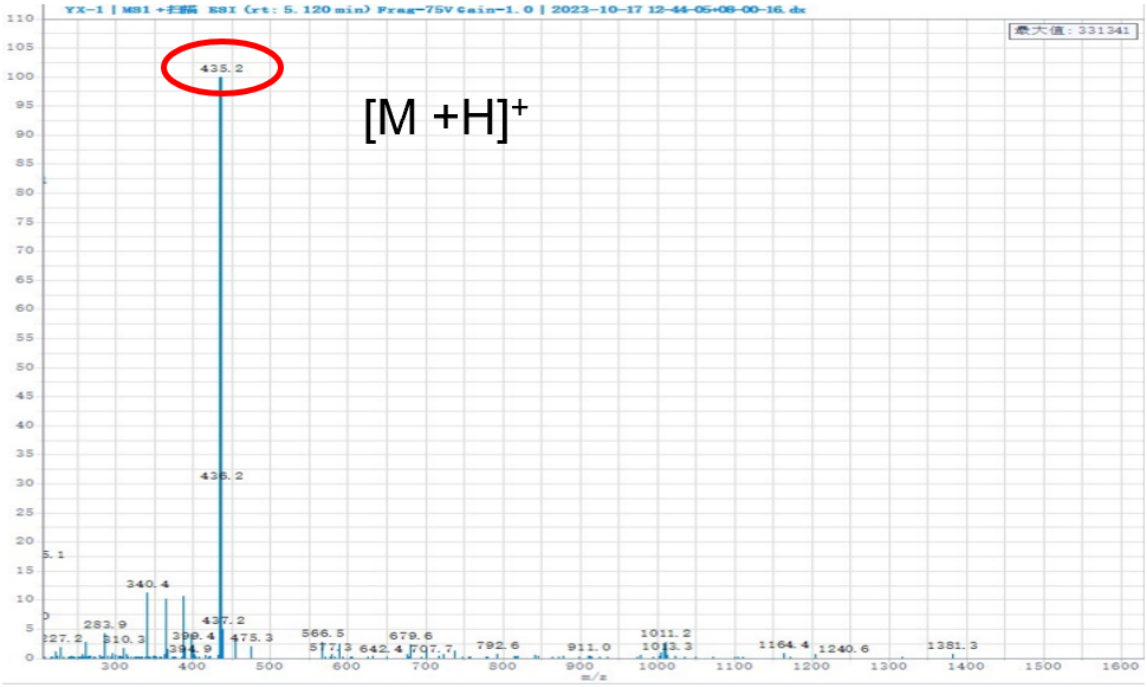

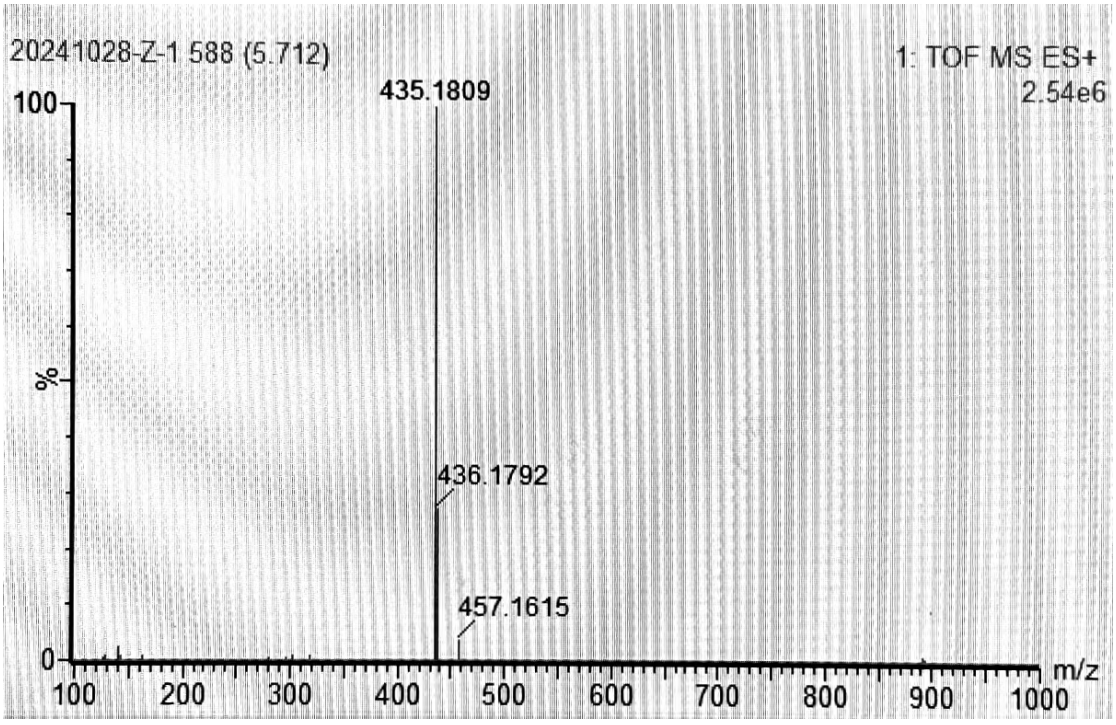

Fig. S3. ESI-MS and HRMS spectrum of **SWJT-OH**.

4. ^{1}H, ^{13}C NMR, ESI-MS and HRMS copies of SWJT-32.

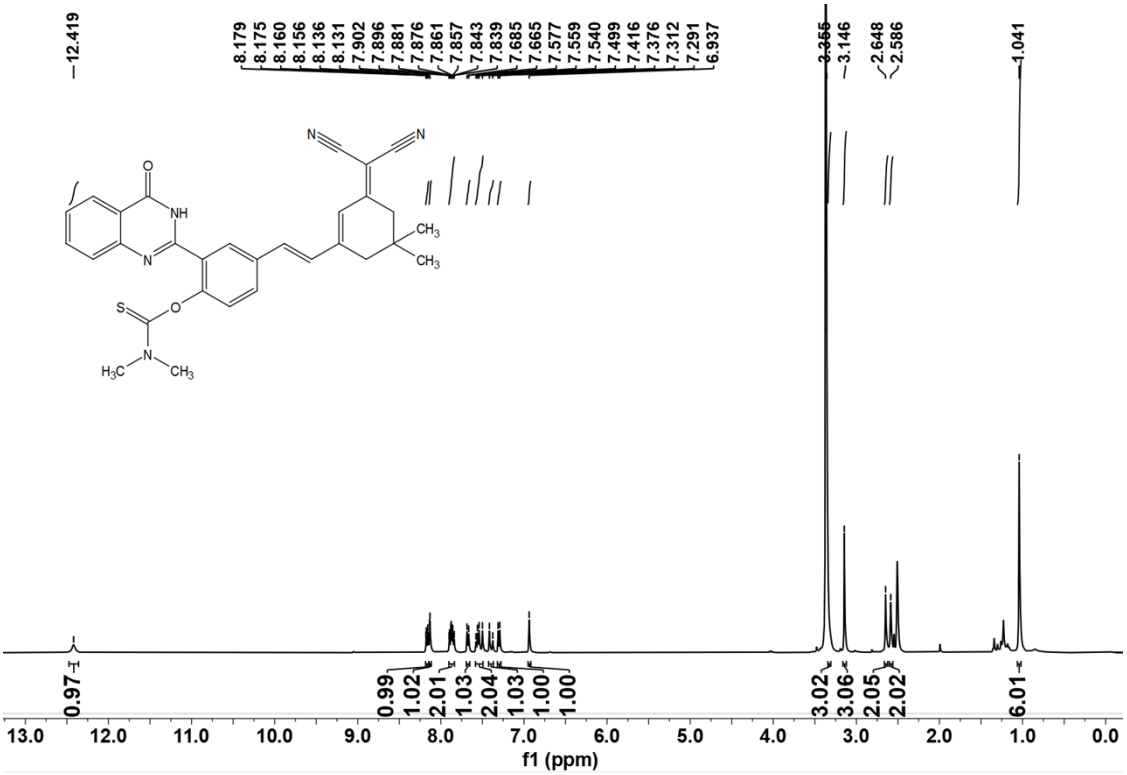

Fig. S4. ^{1}H NMR spectrum of **SWJT-32** in DMSO-d_6 (400MHz).

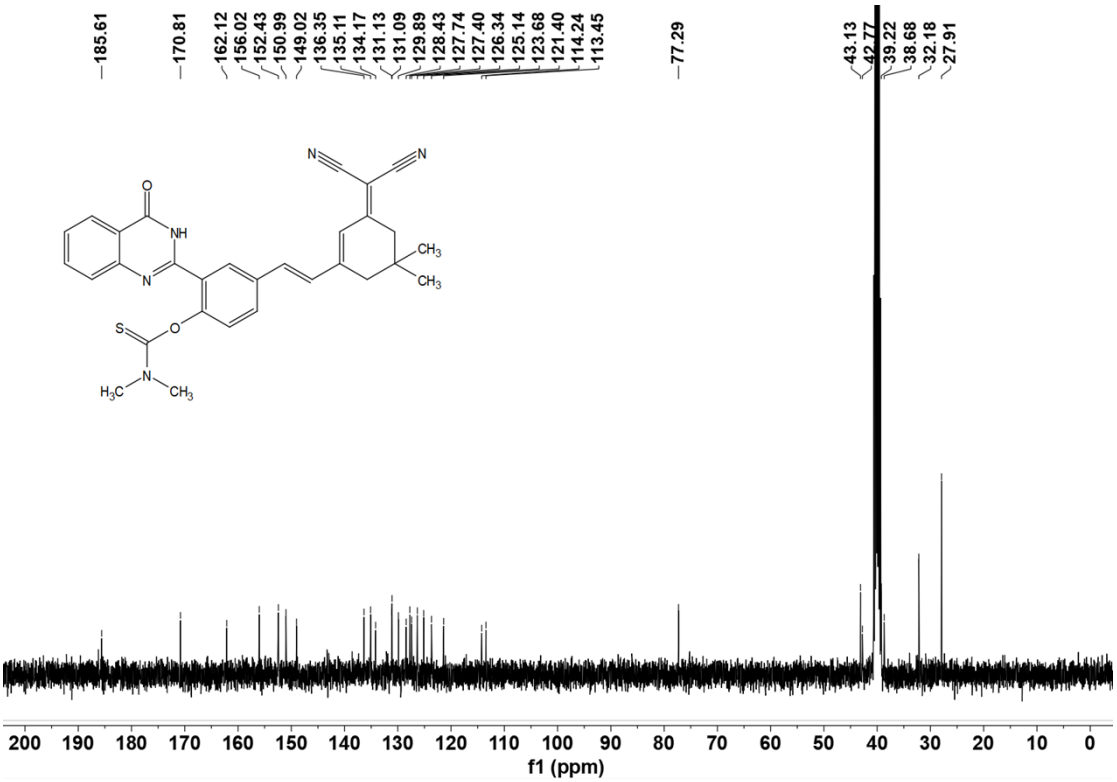

Fig. S5. ^{13}C NMR spectrum of **SWJT-32** in DMSO-d_6 (100 MHz).

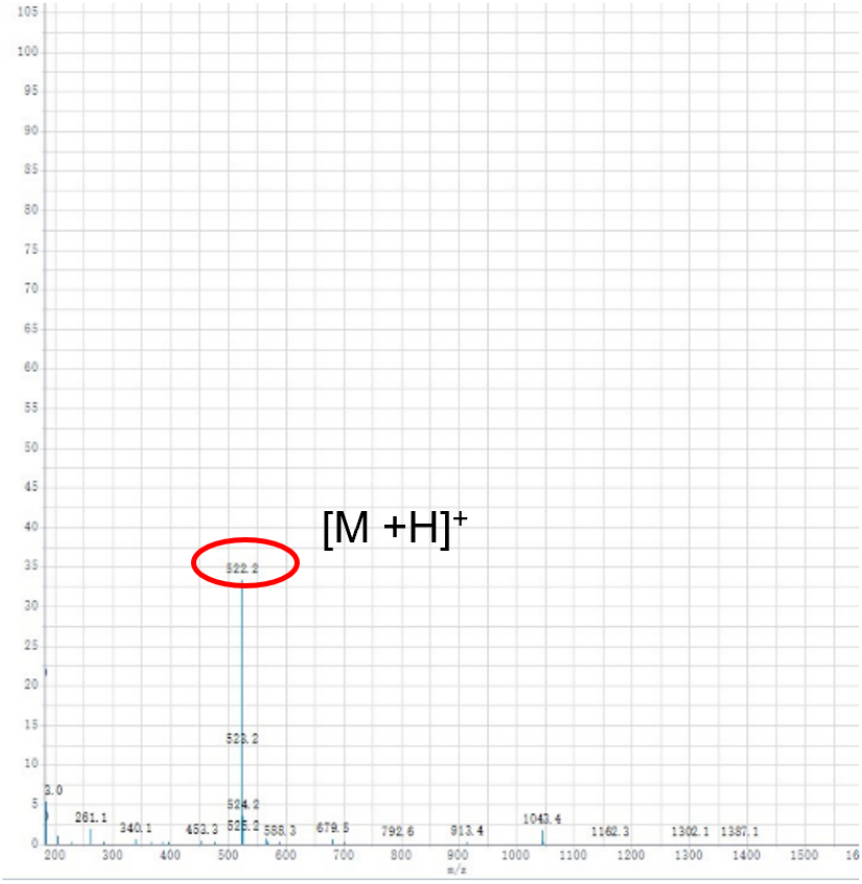

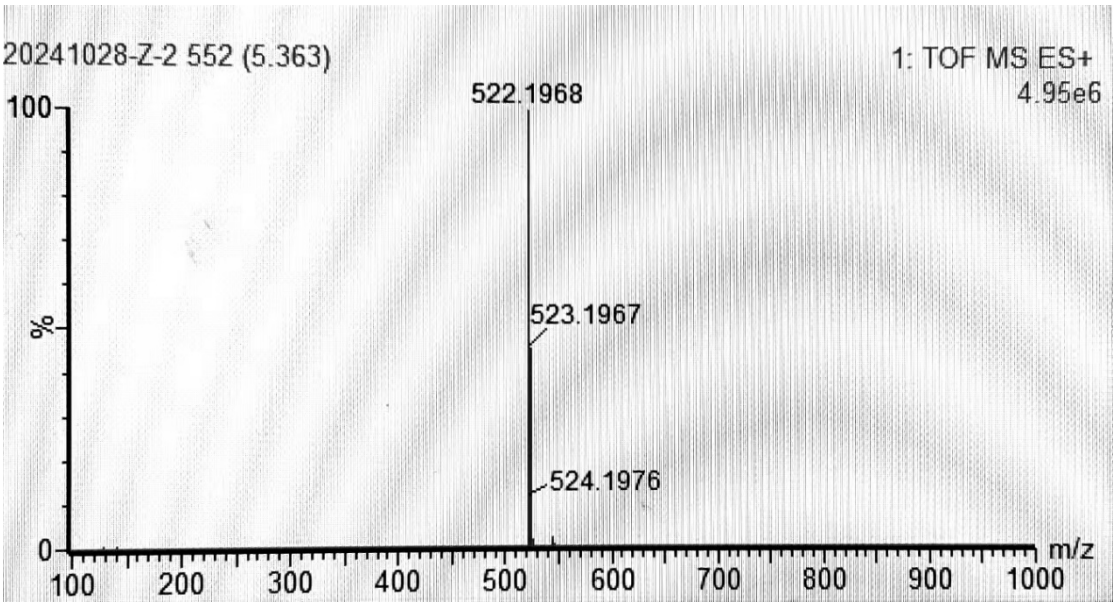

Fig. S6. ESI-MS and HRMS spectrum of **SWJT-32**.

5. ESI-MS spectrum of probe SWJT-32 + ClO⁻.

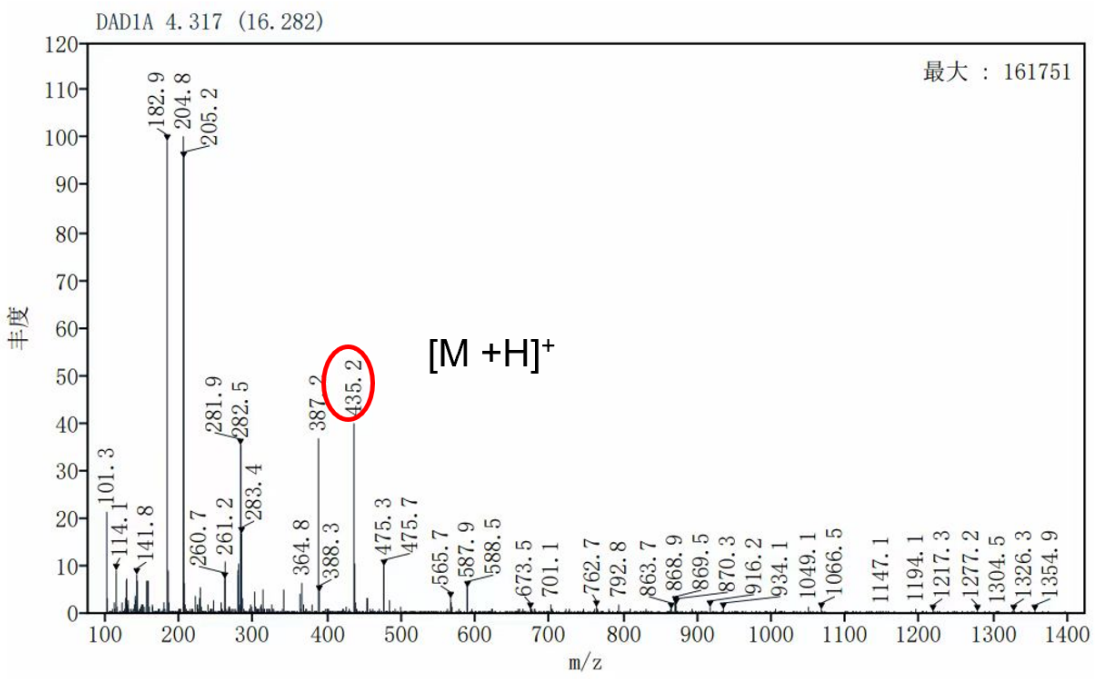

Fig. S7. ESI-MS spectrum of probe **SWJT-32** + ClO⁻.

6. Test condition screening.

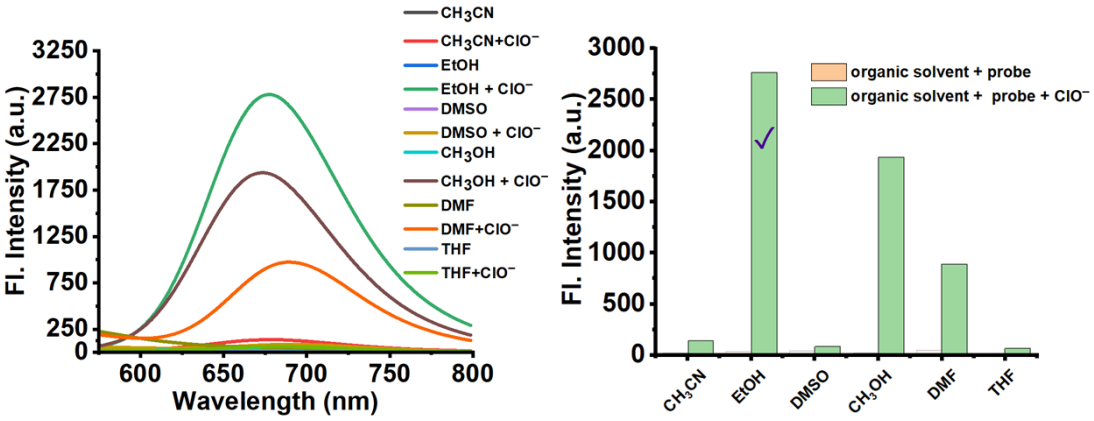

Fig. S8. The effect of different organic solvent on the fluorescence intensity 660 nm of **SWJT-32** (λ_{ex} = 520 nm).

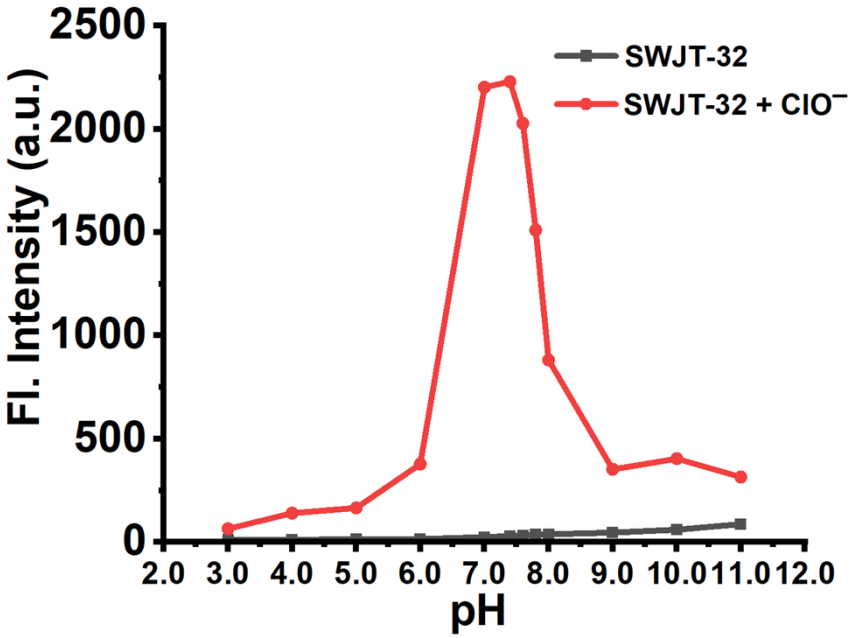

Fig. S9. Fluorescence responses of **SWJT-32** and **SWJT-32** + ClO^- (200.0 μM) under different pH conditions (λ_{ex} = 520 nm).

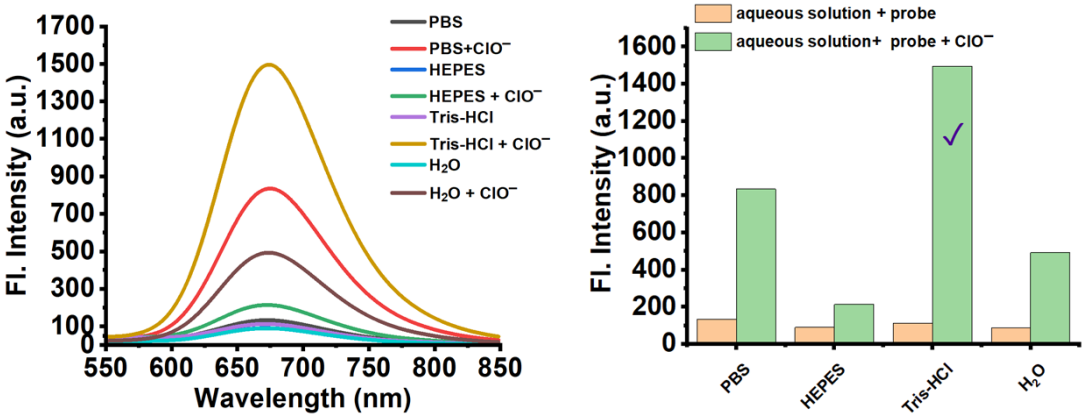

Fig. S10. The effect of different buffer solutions solvent on the fluorescence intensity 660 nm of **SWJT-32** in the absence or presence of ClO^- (λ_{ex} = 520 nm).

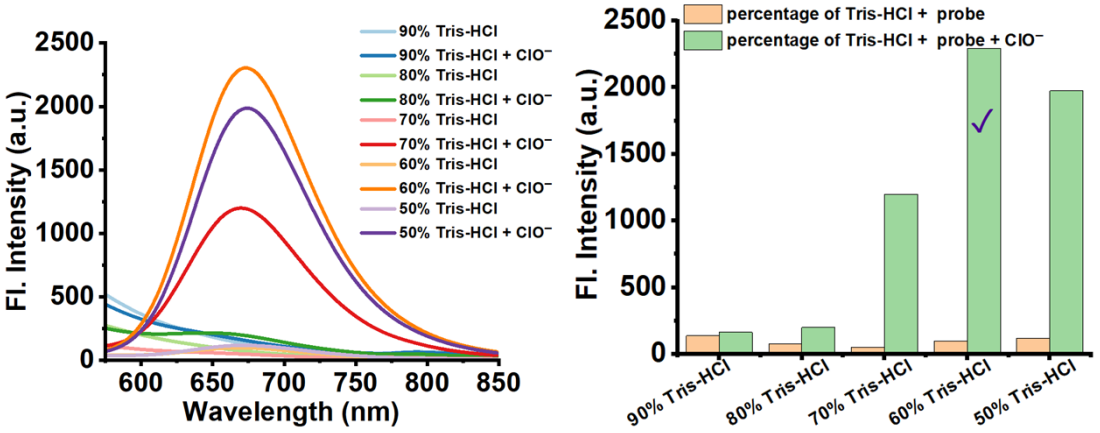

Fig. S11. The effect of different aqueous phase ratios on the fluorescence intensity of **SWJT-32** at 660 nm in the absence or presence of ClO^- (λ_{ex} = 520 nm).

7. The kinetic study of the response of SWJT-32 to ClO⁻.

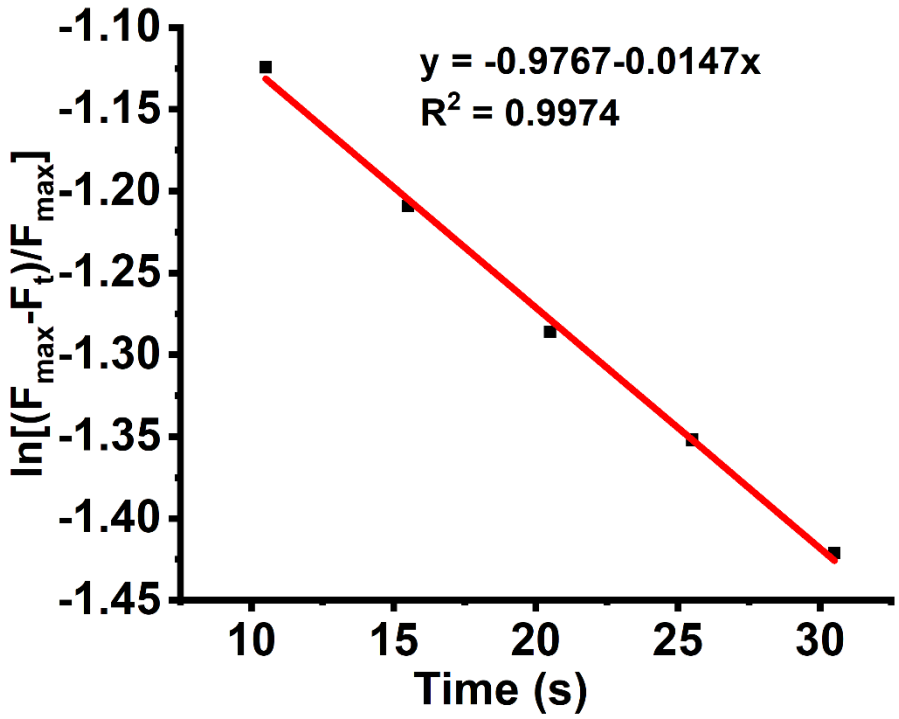

Fig. S12. Pseudo first-order kinetic plots of **SWJT-32** (10.0 μM) with the addition of ClO^- (200.0 μM) (λ_{ex} = 520 nm).

The result of the analysis as follows：

$$\ln [(F_{max}-F_t) / (F_{max})] = k_{obs}t$$

$$t_{1/2} = \ln 2/k_{obs}$$

Where F_{max} and F_t are the fluorescent intensity at time t and initial time. k_{obs} is the pseudo-first-order rate constant.

$$k_{obs} = 1.47 \times 10^{-2}\ s^{-1}$$

8. Detection limit of **SWJT-32** to ClO^-

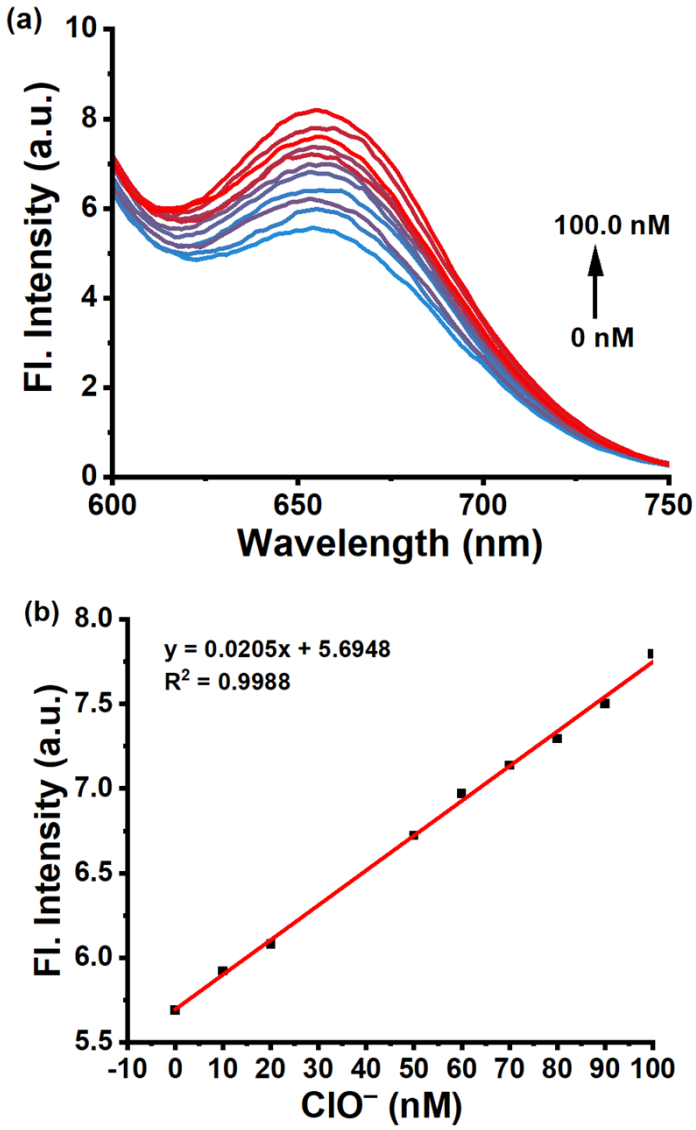

Fig. S13. (a) Fluorescence emission spectra of SWJT-32 (10.0 μM) with the different concentrations of ClO^- (0.0–100.0 nM). (b) The relationship between I_{660nm} and ClO^- concentration in EtOH/Tris-HCl buffer solution (4:6, v/v, pH = 7.4) (λ_{ex} = 520 nm).

The detection limit is calculated according to the formula:

$LOD = 3\sigma/k$

σ: standard deviation of probe blank measurements ($\sigma_{\mathbf{SWJT\text{-}32}}$ = 0.0539).

k: slope of the fluorescence intensity versus concentration plot (k=0.0205).

$LOD = 3\sigma/k$=7.89 nM

9. Cytotoxicity assays.

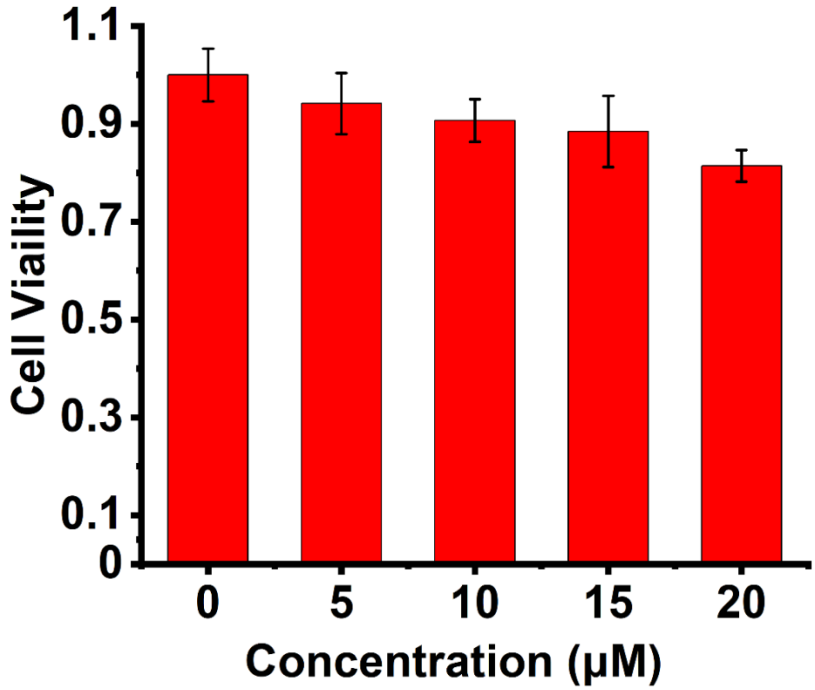

Fig. S14. MTT assay for estimating cell viability of HeLa cells treated with various concentrations of **SWJT-32** (0-20.0 μM) after 24 h incubation.

10. SWJT-32 and compound 1 anti-diffusion test in agarose.

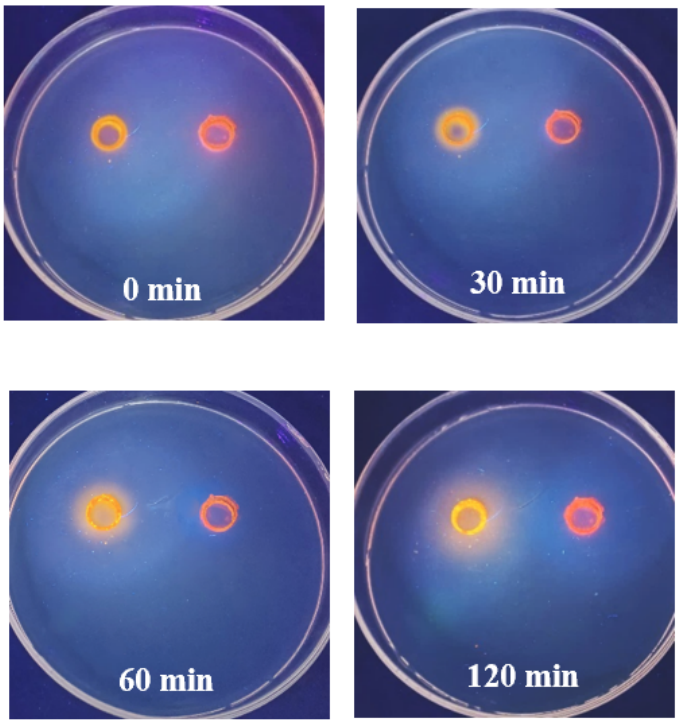

Fig. S15. Diffusion resistance of compound 1 (left ring) and SWJT-OH (right ring) under ultraviolet excitation at 365 nm in agarose.

11. Imaging of tumors and other major organs.

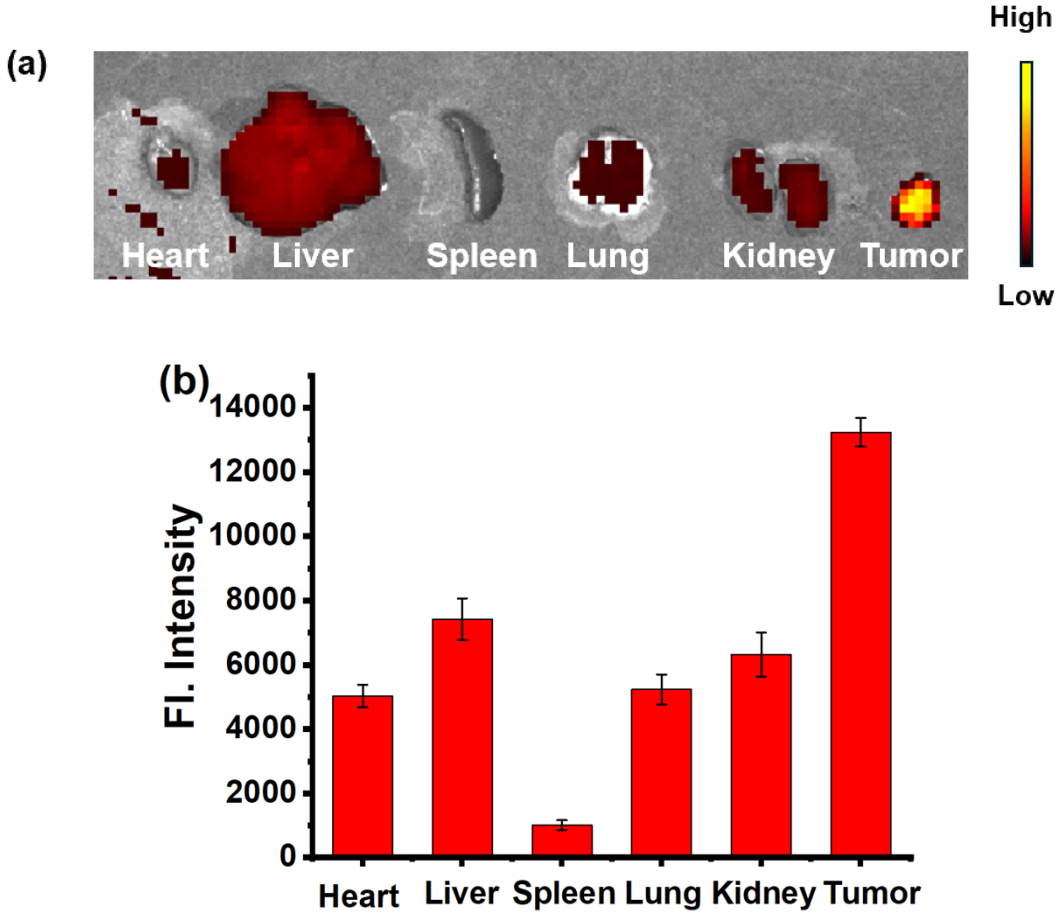

Fig. S16. (a) Fluorescence imaging of tumors and other major organs (heart, liver, spleen, lung, and kidney) after the mice were dissected. (b) Normalized intensity found in (a) (λ_{ex} = 520 nm and λ_{em} = 540-700 nm).